Flexible Molecular Model of Methanol for a Molecular Dynamics Study of Liquid and Supercritical Conditions

Tetsuo Honma,[†,‡] Chee Chin Liew,[§] Hiroshi Inomata,*[,†] and Kunio Arai[†,||]

Research Center of Supercritical Fluid Technology, Tohoku University, Sendai, 980-8579, Japan, Supercritical Fluid Research Center, National Institute of Advanced Industrial Science and Technology (AIST), Sendai, 983-8551, Japan, and Research Institute for Computational Sciences (RICS), National Institute of Advanced Industrial Science and Technology (AIST), Tsukuba, 305-8568, Japan

Received: November 27, 2002; In Final Form: February 24, 2003

A new flexible molecular model of methanol was developed for computer simulations applicable to conditions from the liquid to the supercritical state. The proposed model considered methanol as three interaction sites, oxygen atom, methyl group, and hydrogen atom, and was represented as the sum of intramolecular and intermolecular potentials. The intramolecular potential function introduced a Toukan−Rahman potential and the intermolecular potential function applied an OPLS function. The potential parameters were adjusted to represent the experimental saturated liquid density of methanol at 25 °C. The estimated critical point of the proposed model (T_C = 232.2 °C, ρ_C = 0.278 g·cm^{-3}) was found to be close to the experimental critical point. Transport properties and vibrational spectra were in good agreement with the literature values. The fluid structure of methanol was studied via analyses made on the spatial distribution function. Methanol was found to have chainlike structures in the liquid state and perturbed structure at supercritical conditions. From the analyses, roughly half of the hydrogen bonding molecules in the liquid state were preserved even in supercritical conditions.

Introduction

The structure of hydrogen bonding fluids change greatly when fluid conditions are brought from the ambient state to the supercritical state.[1,2] Many researchers have tried to elucidate the hydrogen bonding structure of fluids at higher temperatures and pressures from neutron diffraction,[1,3] X-ray diffraction,[4,5] and theoretical approaches.[6−9] Theoretical approaches have made much progress in describing hydrogen bonding fluids as evident from the many potentials such as SPC,[10] SPC/E,[11] TIPS,[12] OPLS,[13] and other models.[14−16] Our research group has published a flexible model for water denoted as the cm4p-mTR model,[17] which could accurately represent water's critical properties and its hydrogen bonding behavior in the supercritical region.[18]

Most methanol potentials proposed in the literature are rigid models.[19−21] Jørgensen[13,22] and Haughney et al.[23] originally developed methanol models that reproduced thermodynamic properties and the structure substances in the liquid state. However, despite the importance of the critical region, rigid models have lower critical temperatures compared with the experimental values.[24,25] Molecular flexibility may be an important factor to improve the model capability for representing the critical point, because this is one aspect that allows relaxation of the kinetic energy transfer of molecular collisions. In addition, molecular flexibility can provide vibrational spectra that can make a direct comparison with Raman or infrared spectra. Flexible methanol models have been published by Palinkas,[26,27] which are based on the BJH water model.[28] The Palinkas methanol models can change its dipole moment according to the thermodynamic state and exhibit a gas−liquid frequency shift in the vibrational spectrum. However, the functional form of the model is a sum of the CCL model and unique polynomial functions that requires much effort to compose an aqueous system with the currently used water models. Methanol, like water, can be represented in terms of three sites: oxygen atom, methyl group, and hydrogen atom. In a dilute aqueous solution at ambient liquid conditions, for example, it has been suggested that a methanol molecule could replace a water molecule in a hydrogen bonding network and only slightly perturb the hydrogen bond network structure. In this work, we propose a methanol model based on the cm4p-mTR potential that can be conveniently implemented by representing methanol as three sites. We discuss the model's critical point, vibrational spectra, self-diffusion coefficients, and the simulated fluid structure and hydrogen bonding.

Molecular Model

The proposed model considered the methanol molecule as three sites: an oxygen atom (site 1, O), the methyl group as a whole (site 2, Me), and a hydrogen atom (site 3, H), and was represented as the sum of intramolecular and intermolecular potentials. The intramolecular potential functions were based on the angular form of Toukan−Rahman model for water,[29] which was modified for methanol model. We adopted three intramolecular vibrational modes of methanol: O−Me stretching, O−H stretching and H−O−Me bending. The O−Me stretching and H−O−Me bending were assumed harmonic, because the displacement amplitude of these motions from

* Corresponding author. E-mail: inomata@scf.che.tohoku.ac.jp.
† Tohoku University.
‡ Currently at Supercritical Fluid Research Center.
§ Research Institute for Computational Sciences (RICS), National Institute of Advanced Industrial Science and Technology (AIST).
|| Supercritical Fluid Research Center, National Institute of Advanced Industrial Science and Technology (AIST).

10.1021/jp027578a CCC: $25.00
Published on Web 04/16/2003

TABLE 1: Intramolecular Potential Parameters for the Proposed Methanol Model

$r_{e,12}$/Å	$r_{e,13}$/Å	$\theta_{e,213}$/deg	D_{OH}/kJ·mol^{-1}	α_{13}/Å^{-1}
1.430	0.945	108.5	435.1	2.3083

K_{r12}/kJ·mol^{-1}	β/kJ·mol^{-1}	γ_{12}/kJ·mol^{-1}	γ_{13}/kJ·mol^{-1}	δ/kJ·mol^{-1}
3022.3200	221.1240	139.1369	103.1043	93.2820

TABLE 2: Intermolecular Potential Parameters for the Proposed Methanol Model

interaction site	m/g·mol^{-1}	q/e	ϵ/kJ·mol^{-1}	σ/Å
oxygen	16.000	−0.700	0.7539	3.0645
methyl group	15.034	0.265	1.2307	3.7300
hydrogen	1.008	0.435	0.0100	0.9000

equilibrium geometries was generally small. Consequently, the intramolecular potential functions were expressed as follows:

$$U_{intra} = U_{12} + U_{13} + U_{213} \quad (1)$$

$$U_{12} = K_{r12}\Delta r_{12}^{\ 2} \quad (2)$$

$$U_{13} = D_{OH}(1 - \exp[-\alpha_{13}\Delta r_{13}])^2 \quad (3)$$

$$U_{213} = \frac{1}{2}\beta(\Delta\theta)^2 r_{12}r_{13} + \gamma_{r12\theta} r_{12}\Delta\theta\Delta r_{12} + \gamma_{r13\theta} r_{13}\Delta\theta\Delta r_{13} + \delta(\Delta r_{12}\Delta r_{13}) \quad (4)$$

where D_{OH} is the dissociation energy for the O−H bond. Subscripts 1−3 denote oxygen, the methyl group, and the hydrogen site, respectively. The r_{ij} and Δr_{ij} are separation and displacement from the equilibrium distance between atom i and j, and $\Delta\theta$ is the bending angle for H−O−Me subtracted from the equilibrium angle. The K_{r12}, α_{13}, β, γ_{12}, γ_{13}, and δ are potential parameters that were fitted to reproduce vibrational frequencies in the gas phase[37] independently of intermolecular potential.[29] The determined parameters are listed in Table 1.

The intermolecular potential function used was a three-site OPLS-type[13] potential:

$$U_{inter} = \sum_i \sum_j 4\epsilon_{ij}\left[\left(\frac{\sigma_{ij}}{r_{ij}}\right)^{12} - \left(\frac{\sigma_{ij}}{r_{ij}}\right)^{6}\right] + \frac{q_i q_j}{r_{ij}} \quad (5)$$

where i and j denote each interaction site of the methanol, σ and ϵ are the Lennard-Jones (LJ) parameters, and q and r are the partial charge and the separation between interaction sites, respectively. The original OPLS model neglects a LJ parameter on the hydrogen site. However, in presimulations with the flexible model, we found that large O−H stretching occurred, leading to the dissociation of the O−H bond above a critical point. To prevent this phenomenon, a LJ parameter on the hydrogen site was introduced. Moreover, the LJ parameter on the O site was adjusted to fit the experimental liquid saturated pressure of methanol at 25 °C and 0.787 g·cm^{-3}, which were taken from IUPAC.[30] The determined intermolecular potential parameters are listed in Table 2.

MD simulations were performed with *NVT* ensembles containing 500 methanol molecules. The equations of motion were solved using the velocity Verlet algorithm[31] with a reversible reference system propagator (r-RESPA) algorithm.[32] Time steps were 1 fs for the intermolecular motion and 0.2 fs for the intramolecular motion. The total simulation time was 300 ps including 100 ps equilibration. The first 60 ps of simulation, the temperature was maintained at the desired value with momentum scaling and afterward it was controlled with the Nosé−Hoover thermostat. The electrostatic forces were approximated with a cutoff distance of 10 Å for each interaction pair, and energy contributions outside cutoff cavities were treated with a site−site reaction field method[31,33] with a dielectric continuum. For this study, we chose the four state conditions listed in Table 3, three of which had been the target of structural analysis using neutron diffraction H/D substitution by Yamaguchi et al.[5]

TABLE 3: State Points for Simulation

	supercritical	near-critical	subcritical	liquid
T/°C	245	245	195	25
ρ/g·cm^{-3}	0.716	0.463	0.716	0.787

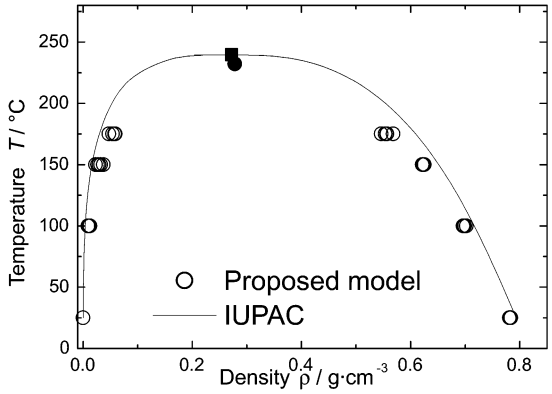

Figure 1. Vapor−liquid coexistence densities. Circles: MD simulation with the proposed model. Filled circle: model's estimated critical point. Solid line: experimental data obtained from IUPAC.[31] Filled square: experimental critical point.

TABLE 4: Critical Temperature and Density of the Proposed Model and Literature

	proposed	OPLS[24]	OPLS[25]	IUPAC[31]
T_C/°C	232.2	220	211.5	239.5
ρ_C/g·cm^{-3}	0.278	0.25	0.262	0.279

TABLE 5: Peak Frequencies in Vibrational Spectra

	libration	Me−O stretching	Me−O−H bending	O−H stretching
supercritical	245	1028	1240	3530
subcritical	193	1025	1240	3590
near-critical	485	1028	1248	3508
liquid	560	1033	1305	3440
liquid (harmonic)	560	1033	1308	3705
exp values[38]				
liquid	655	1029	1420	3337
gas		1034	1346	3687

Critical Properties of Proposed Methanol Model

We estimated the vapor−liquid saturated densities of the proposed model with a direct simulation technique of Alejandre et al.[34] to examine its performance as a methanol model in the subcritical and supercritical region. The obtained vapor−liquid saturated densities are shown in Figure 1. The data had fluctuations in the vicinity of the critical point, but they were in agreement with the saturation data of IUPAC.[30] The critical point of the proposed model was estimated by fitting the coexisting density data using the law of rectilinear diameters and the scaling law with a scaling exponent of 0.325.[35] The critical temperature and density obtained from the proposed flexible model are listed in Table 4. The proposed model was found to reproduce the critical point better than the results of

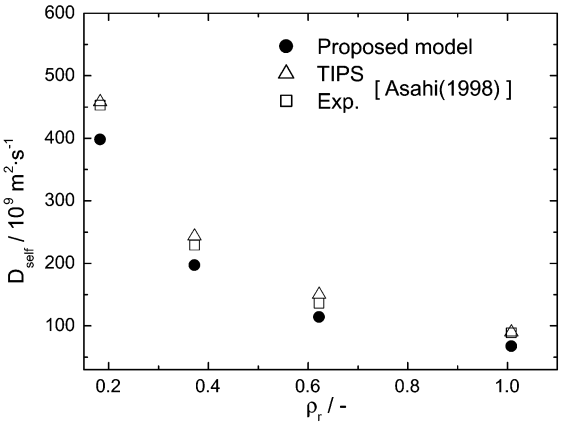

Figure 2. Dependence of self-diffusion coefficient on the densities. Filled circles: estimated from MD simulation of proposed model. Open squares: NMR data.[36] Open triangles: MD simulation[36] (TIPS model).

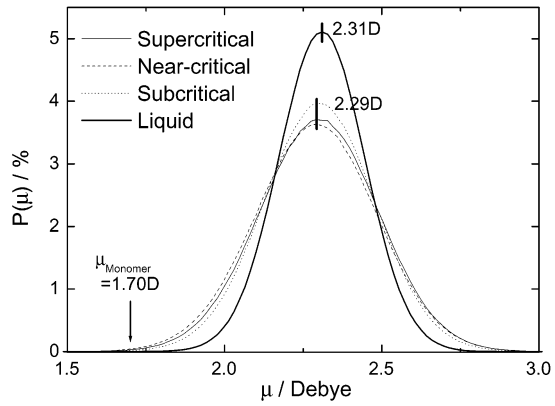

Figure 3. Dipole moment distribution of proposed model.

the current rigid OPLS model,[24,25] which may be attributed to the molecular flexibility that allows relaxation of kinetic energies.

The self-diffusion coefficient, D_{self}, was calculated from the mean square displacement (MSD):

$$D_{self} = \lim_{t\to\infty} \frac{1}{6t} \langle |r(t) - r(0)|^2 \rangle \qquad (6)$$

where $r(t)$ is the position vector at time t. The maximum time for estimating MSD was 0.2 ps, which made MSD a constant slope and was enough time to compute the self-diffusion coefficient. The density dependence of the self-diffusion coefficient determined from the proposed model at a reduced temperature of $T_r = 1.15$ is shown in Figure 2. For comparison, the self-diffusion coefficients of Asahi and Nakamura[36] via MD simulation of the TIPS model and ^{1}H NMR spin−echo techniques measurement are also shown in Figure 2. The self-diffusion coefficient decreased with increasing density, which was qualitatively consistent. However, the proposed model underestimated the self-diffusion coefficient at low densities compared with the literature values, which may be attributed to the TIPS methanol model having about a 10% lower critical temperature.[19]

Figure 3 shows the dipole moment distribution in terms of the density for the proposed model. In the liquid state, the distribution ranged from 1.7 to 3.0 D with the maximum population being around 2.3 D. This was different from that determined by Palinkas et al.[26] and could be attributed to differences in monomer geometries. At higher temperatures, the distributions of the proposed methanol model tended to follow

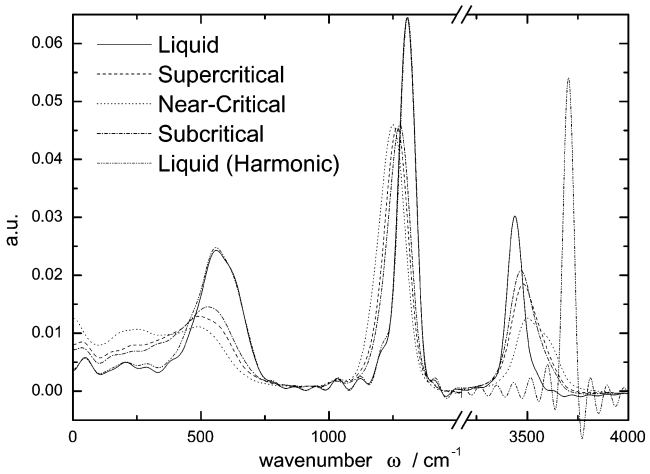

Figure 4. Power spectra of velocity autocorrelation function for H-site.

the Boltzmann distribution, suggesting the validity of the simulation near the critical point.

Power spectra for vibrational modes of three sites of methanol model, $I(\omega)$, were obtained as a Fourier transform of the velocity autocorrelation function as follows:

$$I(\omega) = \int_0^\infty \frac{v(t)\, v(0)}{v(0)\, v(0)} \cos(\omega t)\, dt \qquad (7)$$

where $v(t)$ is the velocity of each atom at time t and ω is the wavenumber. Harmonic potential for O−H vibration was applied to examine the effect of unharmonicity for the intramolecular potential. The peak frequencies of vibrational mode and power spectra for the hydrogen site are shown in Table 5 and Figure 4.

The peak frequencies around 600, 1030, 1250, and 3500 cm^{-1} were assigned as libration, Me−O vibration, Me−O−H bending, and O−H vibration, respectively. Falk and Whalley obtained a gas−liquid frequency shift by infrared spectroscopy that was 250 cm^{-1}.[37] In our simulation, there was a 250 cm^{-1} difference for O−H vibration between the anharmonic (3450 cm^{-1}, liquid) and the harmonic potential (3700 cm^{-1}, liquid harmonic). Molecular anharmonicity permitted a large O−H separation with hydrogen bonding and a red shift of vibrational frequencies.

At higher temperatures, the Me−O and the Me−O−H bending vibrations shifted to lower frequencies. Koda et al. measured Raman spectral shifts at temperatures from ambient to supercritical state and the C−O stretching frequencies decreased with increasing temperature.[38] The vibrational spectra of the proposed model were in good agreement with the experimental data by Koda et al. However, the simulated Me−O frequencies at higher temperatures were not as sensitive to temperature and density as the experimental values. The O−H vibration was composed of the lower (3450 cm^{-1}) and higher (3600 cm^{-1}) vibration peaks. It should be noted that these two peaks were attributed as hydrogen-bonded molecules and nonbonded monomers, respectively, which implied the hydrogen-bonding structure still remained in the critical regions. The vibrational spectra can provide the qualitative degree of hydrogen bonding according to fluid conditions. However, we chose to use the three-dimensional pair distribution function, so-called spatial distribution function, to obtain detailed hydrogen-bonding information such as orientation and coordination.

Fluid Structure

Three-dimensional analysis with a spatial distribution function was conducted for studying fluid structure around an anisotropic

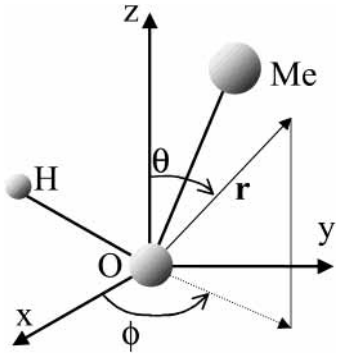

Figure 5. Principal frame coordinates of methanol.

molecule such as methanol. In this study, the definition of the principal frame coordinates described by Svishchev and Kusalik was adopted.[39] As defined in Figure 5, **r** is a position vector pointing toward a site of another molecule from the oxygen site, θ is the angle between the vector **r** and a *z*-axis bisecting the angle Me−O−H, and ϕ is the angle between the *x*-axis and the **r**-projection onto the $x-y$ plane. The spatial distribution function at $\theta = 0-360°$ and $\phi = 0°$ was chosen for analysis. According to the definition, it can be expected that linear hydrogen bonding will be observed at $r = 2.8$ Å, $\theta = 60°$, and $\phi = 0°$ defined as LHB1 and $r = 2.8$ Å, $\theta = 180°$, and $\phi = 0°$ defined as LHB2 and an area around methyl group $\theta = 300°$ and $\phi = 360°$.[39]

The oxygen−oxygen spatial distribution function estimated from the proposed model, g_{OO}, in the liquid state is shown in Figure 6a. We also performed additional simulations with the original OPLS model, shown in Figure 6b, which yielded a comparable spatial distribution function. For the case of the first shell, two sharp peaks occurred at LHB1 and LHB2. The peak height at LHB1 for the proposed model was about 130 times higher than that estimated from bulk density. The second solvation shell could be seen at $r = 4.5$ Å, $\theta = 30°$, 90°, and 150°, and broader a third solvation shell occurred at $r = 7$ Å and $\theta \leq 240°$. The two main peaks of the first solvation shell come from linear hydrogen bonding that bound strongly each other. It should be noted that the LHB1 peak of the proposed model was slightly higher than that of the rigid OPLS model. This means that that molecular flexibility changes the molecule's dipole moment and it might promote formation of hydrogen bonding. In the second solvation shell, two peaks at $\theta = 30°$ and 120° at the same separations imply a chainlike structure proposed by Jørgensen.[22] The peak at $\theta = 90°$ relates branches in the chainlike structure. Around the methyl group, it could be seen that only one broad peak was present at $r = 4-7$ Å and $\theta \geq 180°$. The methyl group has a large exclusive volume, and this probably leads to the formation of chainlike structures of methanol rather than three-dimensional networks.

Figure 7a and Figure 7b show spatial distribution functions at supercritical conditions ($T = 245$ °C, $\rho = 0.716$ g·cm^{-3}) obtained from the proposed model and the rigid OPLS model, respectively. The structure obtained from the proposed model was qualitatively in agreement with that determined from the original OPLS model and the neutron diffraction data with H/D substitution treatment estimated by Yamaguchi et al.[5] Two clear peaks occurred at LHB1 and LHB2 and became much broader and lowered compared with those in the liquid state. The hydrogen bonding fluctuated but still remained at supercritical condition, but no long-range liquid structural features such as chainlike structures could be observed. The second shell, $r = 4.5$ Å, and third shell, $r = 7$ Å, were different and significantly smaller than that in the liquid state. We also estimated the g_{OO}

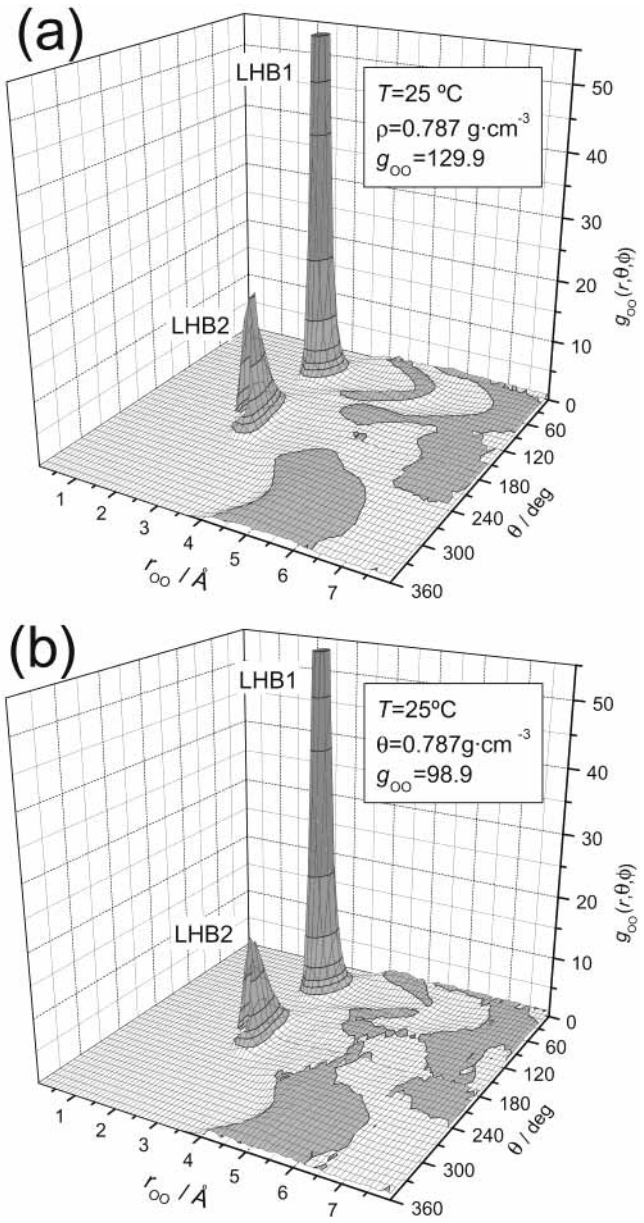

Figure 6. Spatial distribution function in the liquid state. (a) Proposed model. (b) Rigid OPLS model.

at $\phi = 90°$ for methanol, which was perpendicular to its molecular plane. In this plane at $r = 2.8$ Å and $\theta = 180°$ exhibited one peak, which was the same as the peak at LHB2. Therefore, we confirmed that the methanol model could coordinate up to two molecules at LHB1 and LHB2.

For quantitatively discussing the state condition dependence of the hydrogen bonding, we evaluated the average number of hydrogen bonds per molecule. There have been many criteria of hydrogen bonding: geometric definitions,[3,40] energetic definitions,[12,41] and combinations of these.[42,43] In this work, we adopted the geometric definition by Yamaguchi et al.[5] to compare our results with their data. The hydrogen bond between two molecules was defined as follows:

$$2.0 \text{ Å} \leq r_{O\cdots O} \leq 3.4 \text{ Å}$$
$$1.4 \text{ Å} \leq r_{O\cdots H} \leq 2.4 \text{ Å} \quad (8)$$

where $r_{O\cdots O}$ and $r_{O\cdots H}$ are oxygen−oxygen and oxygen−hydrogen separations, respectively. The estimated average numbers of the hydrogen bond are listed in Table 6. The values

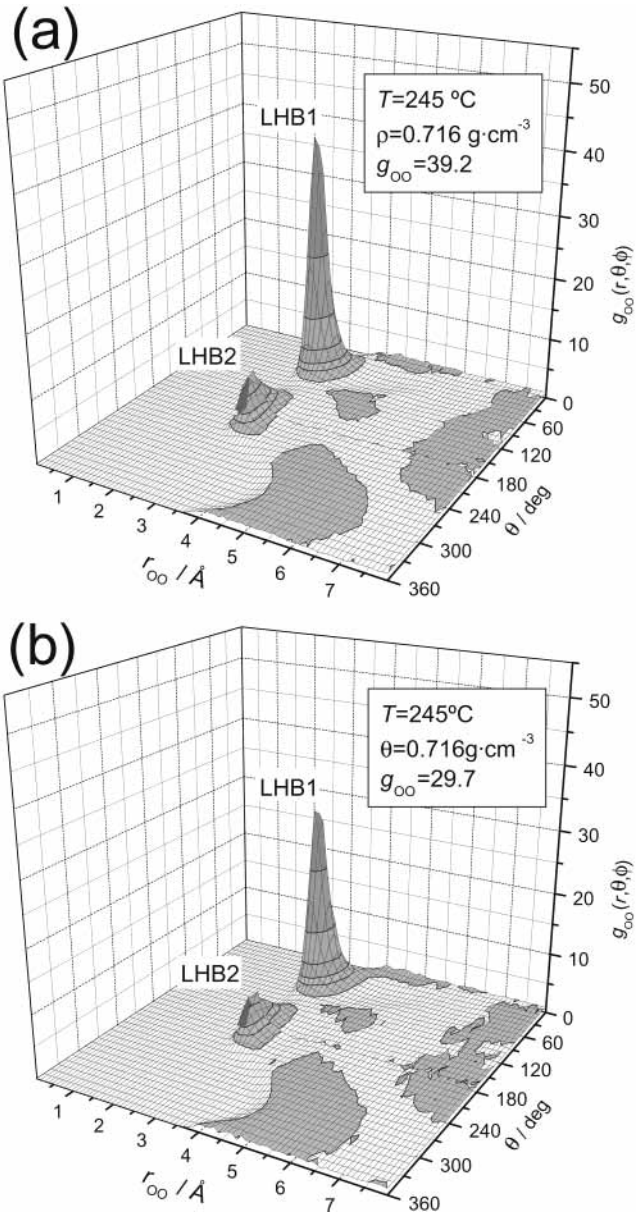

Figure 7. Spatial distribution function in supercritical state. (a) Proposed model. (b) Rigid OPLS model.

TABLE 6: Hydrogen Bonding Analysis From the Geometric Criteria (See Text)[a]

	proposed	rigid OPLS	ref 5	ref 45
liquid	1.90	1.83	1.77	(1.0)
supercritical	1.30 (0.68)	1.16 (0.64)	1.6 (0.90)	(N/A)
near-critical	0.98 (0.52)	0.89 (0.49)	1.0 (0.56)	(0.4)
subcritical	1.43 (0.75)	1.29 (0.71)	1.6 (0.90)	(0.6−0.8)

[a] Values in parentheses are normalized values with the value at liquid state.

in brackets are normalized with the liquid state value. The number of hydrogen bonds at each state point showed that the hydrogen bonding decreased with decreasing density and increasing temperature, as expected. At high temperature conditions, roughly half the number of hydrogen bonds still remained compared with that in the liquid state. The average number of hydrogen bonds obtained from the proposed model were 10% higher than those from the original OPLS model, which may be due to the model's temperature dependence of the dipole moment and its flexible nature that contributes to relaxation of kinetic energies. Table 6 contains values by Yamaguchi et al. from the spatial distribution functions from MD simulations of the empirical potentials tuned by the structure refinement approach.[5] They were 1.6, 1.0, and 1.6 at the supercritical, the near-critical, and the subcritical conditions, respectively. In addition, the values determined by Hoffman and Conradi from the ^{1}H NMR chemical shift[44] are also tabulated. Although the average numbers of hydrogen bonding estimated from the proposed model were up to 20% lower than those by Yamaguchi et al., and there are 30% variations in values among researchers. Simulations with the proposed flexible model could represent the qualitative tendency of hydrogen bonding at higher temperatures and probably provides a better estimation of the true solution structure.

Conclusions

A new flexible methanol model was developed that used an angular form of the TR intramolecular and the OPLS intermolecular potentials. The LJ parameter on the H-site prevented dissociation at supercritical conditions, especially higher density conditions. The critical point of the proposed model ($T_C = 232.2$ °C, $\rho_C = 0.278$ g·cm^{-3}) was in good agreement with experimental values and provides reliability of the chosen simulation thermodynamic state of methanol, especially at supercritical conditions. The fluid structure of a proposed model had a qualitative agreement with the current model and experiment. In the liquid state, a chainlike structure was formed, but it was perturbed in the critical region. We evaluated the average number of hydrogen bonds via a geometric criteria, it was qualitatively well-reproduced trend and was quantitatively in an error range up to 30% from the literatures. More than half of hydrogen bonds are still preserved in the critical regions according to present simulations. The proposed flexible methanol model could be applied to study supercritical systems and those at extreme conditions of temperature and pressure.

Acknowledgment. This work has been partly supported by CREST of JST (Japan Science and Technology).

References and Notes

(1) Soper, A. K. *Chem. Phys.* **2000**, *258*, 121−137.
(2) Chialvo, A. A.; Yezdimer, E.; Driesner, T.; Cummings, P. T.; Simonson, J. M. *Chem. Phys.* **2000**, *258*, 109−120.
(3) Soper, A. K.; Bruni, F.; Ricci, M. A. *J. Chem. Phys.* **1997**, *106* (1), 247−254.
(4) Yamaguchi, T. *J. Mol. Liq.* **1998**, *78*, 43−50.
(5) Yamaguchi, T.; Benmore, C. J.; Soper, A. K. *J. Chem. Phys.* **2000**, *112* (20), 8976−8987.
(6) Chialvo, A. A.; Cummings, P. T. *J. Chem. Phys.* **1994**, *101* (5), 4466−4469.
(7) Chalaris, M.; Samios, J. *J. Phys. Chem. B* **1999**, *103* (7), 1161−1166.
(8) Jedlovszky, P. *J. Chem. Phys.* **2000**, *113* (20), 9113−9121.
(9) Predota, M.; Nezbeda, I.; Cummings, P. T. *Mol. Phys.* **2002**, *100* (14), 2189−2200.
(10) Berendsen, H. J. C.; Postma, J. P. M.; van Gunsteren, W. F.; Hermans, J. *Intermolecular Forces*; Pullman, B., Ed.; Reidel: Dordrecht, The Netherlands, 1981.
(11) Berendsen, H. J. C.; Grigerarand, J. R.; Straatsma, T. P. *J. Phys. Chem.* **1987**, *91* (24), 6269−6271.
(12) Jørgensen, W. L.; Chandrasek, J.; Madura, J. D.; Impey, R. W.; Klein, M. L. *J. Chem. Phys.* **1983**, *79* (2), 926−935.
(13) Jørgensen, W. L. *J. Phys. Chem.* **1986**, *90* (7), 1276−1284.
(14) Sprik, M.; Klein, M. L. *J. Chem. Phys.* **1988**, *89* (12), 7556−7560.
(15) Rick, S. W.; Stuart, S. J.; Berne, B. J. *J. Chem. Phys.* **1994**, *101* (7), 6141−6156.
(16) Svishchev, I. M.; Kusalik, P. G.; Wang, J.; Boyd, R. J. *J. Chem. Phys.* **1996**, *105* (11), 4742−4750.

(17) Liew, C. C.; Inomata, H.; Arai, K. *Fluid Phase Equilibr.* **1998**, *144*, 287−298.
(18) Liew, C. C.; Inomata, H.; Arai, K.; Saito, S. *J. Supercrit. Fluids* **1998**, *13*, 83−91.
(19) van Leeuwen, M. E.; Smit, B. *J. Phys. Chem.* **1995**, *99* (7), 1831−1833.
(20) Bakó, I.; Jedlovszky, P.; Pálinkas, G. *J. Mol. Liq.* **2000**, *87*, 243−254.
(21) Walser, R.; Mark, A. E.; van Gunsteren, W. F.; Lauterbach, M.; Wipff, G. *J. Chem. Phys.* **2000**, *112* (23), 10450−10459.
(22) Jørgensen, W. L. *J. Am. Chem. Soc.* **1981**, *103* (2), 335−340.
(23) Haughney, M.; Ferrario, M.; McDonald, I. R. *Mol. Phys.* **1986**, *58* (4), 849−853.
(24) Mezei, M. *Mol. Simul.* **1992**, *9* (4), 257−267.
(25) Kettler, M.; Nezbeda, I.; Chialvo, A. A.; Cummings, P. T. *J. Phys. Chem. B* **2002**, *106* (30), 7537−7546.
(26) Palinkas, G.; Hawlicka, E.; Heinzinger, K. *J. Phys. Chem.* **1987**, *91* (16), 4334−4341.
(27) Hawlicka, E.; Palinkas, G.; Heinzinger, K. *Chem. Phys. Lett.* **1989**, *154* (3), 255−259.
(28) Bopp, P.; Janscó, G.; Heinzinger, K. *Chem. Phys. Lett.* **1983**, *98*, 129−133.
(29) Toukan, K.; Rahman, A. *Phys. Rev. B* **1985**, *31* (5), 2643−2648.
(30) de Reuck, K. M., Craven, R. J. B., Eds. *Methanol*, IUPAC Chemical Data Series; Blackwell Science Inc.: Glasgow, 1993.
(31) Allen, M. P.; Tildesley, D. J. *Computer Simulation of Liquids*, 2nd ed.; Oxford University Press Inc.: Oxford, U.K., 1987.
(32) Tuckerman, M.; Berne, B. J.; Martyna, G. J. *J. Chem. Phys.* **1992**, *97* (3), 1990−2001.
(33) Hummer, G.; Soumpasis, D. M.; Neumann, M. *Mol. Phys.* **1992**, *77* (4), 769−785.
(34) Alejandre, J.; Tildesley, D. J.; Chapela, G. A. *J. Chem. Phys.* **1995**, *102* (11), 4574−4583.
(35) Guissani, Y.; Guillot, B. *J. Chem. Phys.* **1993**, *98* (10), 8221−8235.
(36) Asahi, N.; Nakamura, Y. *J. Chem. Phys.* **1998**, *109* (22), 9879−9887.
(37) Falk, M.; Whalley, E. *J. Chem. Phys.* **1961**, *34* (5), 1554−1568.
(38) Ebukuro, T.; Takami, A.; Oshima, Y.; Koda, S. *J. Supercrit. Fluids* **1999**, *15*, 73−78.
(39) Svishchev, I. M.; Kusalik, P. G. *J. Chem. Phys.* **1994**, *100* (7), 5165−5171.
(40) Mezei, M.; Beveridge, D. L. *J. Chem. Phys.* **1981**, *74* (1), 622−632.
(41) Petsche, I. B.; Debenedetti, P. G. *J. Chem. Phys.* **1989**, *91* (11), 7075−7084.
(42) Liew, C. C.; Inomata, H.; Saito, S. *Fluid Phase Equilib.* **1995**, *104*, 317−329.
(43) Kalinichev, A. G.; Bass, J. D. *J. Phys. Chem. A* **1997**, *101* (50), 9720−9727.
(44) Hoffmann, M. M.; Conradi, M. S. *J. Phys. Chem. B* **1998**, *102* (1), 263−271.